JOURNAL OF AIRCRAFT
Vol. 32, No. 2, March–April 1995

Finite State Induced Flow Models Part II: Three-Dimensional Rotor Disk

David A. Peters*
Washington University, St. Louis, Missouri 63130
and
Cheng Jian He†
Advanced Rotorcraft Technology, Mountain View, California 94043

In Part I of this two-part article, we developed a finite state induced flow model for a two-dimensional airfoil. In this second part, we develop a finite state induced flow model for the three-dimensional induced flow for a rotor. The coefficients of this model are found in a compact closed form. Although the model does not presuppose anything about the source of lift on the rotating blades, applications are given in which the Prandtl assumption is invoked. That is, the two-dimensional lift equations are used at each radial station, but with the inflow from the three-dimensional model. The results are shown to reduce (in several special cases) to Prandtl–Goldstein theory, Theodorsen theory, Loewy theory, dynamic inflow, and blade-element momentum theory. Comparisons with vortex-filament models and with experimental data in hover and forward flight also show excellent correlation.

Nomenclature

a_j^r, b_j^r = induced inflow expansion coefficients
$\bar{b}$ = nondimensional semichord, $\bar{c}/2$
$\hat{b}$ = locally normalized semichord, $\bar{b}/\bar{r}$
C_n^m, D_n^m = arbitrary coefficients of pressure function
$\bar{c}$ = blade chord nondimensionalized on R
c_j^r, d_j^r = induced inflow coefficients in terms of $\bar{P}_j^r(\nu)$ expansion
$E[\ ]$ = inflow acceleration operator
H_n^m = factorial combination, defined in Eq. (43)
J_n = Bessel function of first kind of order n
j, n = polynomial number
k = reduced frequency, for rotor blade, $\bar{\omega}\bar{b}/\bar{r}$
k_m = $\bar{m}\bar{b}/\bar{r}$
$L[\ ]$ = quasisteady inflow operator
$[L^c]$, $[L^s]$ = cosine and sine part of L operator
$\bar{L}_q$ = circulatory lift of qth blade, dimensionless on $\rho\Omega^2R^3$
$[\hat{L}_{jn}^{rm}]^c$, $[\hat{L}_{jn}^{rm}]^s$ = cosine and sine part of induced inflow influence coefficients associated with radial expansion $\bar{P}_j^r(\nu)$
$[\bar{L}_{jn}^{rm}]^c$, $[\bar{L}_{jn}^{rm}]^s$ = cosine and sine part of induced inflow influence coefficients associated with radial expansion $\bar{\phi}_j^r$
$\bar{L}_y$ = total nondimensional lift
M = total number of harmonics
$[M]$ = apparent mass matrix
m, r = harmonic number
$(n)!!$ = double factorial of n, $(n)(n-2)(n-4)\cdots(2)$, for n even; $(n)(n-2)(n-4)\cdots(1)$, for n odd
P = pressure across disk, dimensionless on $\rho\Omega^2R^2$
P_n^m = associated Legendre functions of first kind
$\bar{P}_n^m$ = normalized Legendre functions, $\bar{P}_n^m(\nu) = (-1)^m P_n^m(\nu)/\rho_n^m$
Q = number of blades
Q_n^m = associated Legendre functions of second kind
$\bar{Q}_n^m$ = normalized Legendre functions, $\bar{Q}_n^m(i\eta) = Q_n^m(i\eta)/Q_n^m(i0)$
q = blade index
q_i = ith component of perturbation velocity, dimensionless on ΩR
R = rotor radius, m
$\bar{r}$ = blade radial coordinate nondimensionalized on R
S = total number of inflow states
$\bar{t}$ = nondimensional time, Ωt
u_0 = inplane velocity relative to airfoil, dimensionless on ΩR
V = flow parameter, dimensionless on ΩR
V_∞ = freestream speed, dimensionless on ΩR
V_n^m = mass flow elements, Eq. (66)
V_T = total flow at rotor plane, dimensionless on ΩR
w = normal component of induced inflow, positive downward, dimensionless on ΩR
w_0, w_1, w_2 = Glauert coefficients of flow normal to airfoil, dimensionless on ΩR
X = function of wake skew angle, $\tan|\chi/2|$
x, y, z = rotor disk coordinates, nondimensionalized on R
x_w, y_w, z_w = wind coordinates, nondimensionalized on R
$\bar{y}$ = chordwise coordinate centered at midchord, dimensionless on R
$(0)!!$ = double factorial of 0, defined as equal to 1
α = angle between freestream and rotor disk, positive nose down
α_e = effective disk angle of attack, $\tan^{-1}(\lambda/\mu)$
α_j^r, β_j^r = induced inflow coefficients in terms of $\phi_j^r(\bar{r})$ expansion
$\bar{\alpha}_j^r$, $\bar{\beta}_j^r$ = induced inflow coefficients in terms of $\bar{\phi}_j^r(\bar{r})$ expansion

Received Sept. 13, 1993; revision received May 23, 1994; accepted for publication June 17, 1994.

*Professor and Director, Center for Computational Mechanics, Campus Box 1129. Fellow AIAA.
†Senior Engineer, 1685 Plymouth St., Suite 250. Member AIAA.

$\bar{\tilde{\alpha}}_1^0$ = steady value of $\tilde{\alpha}_1^0$
λ = total inflow, $\lambda_f + \lambda_m$
λ_f = freestream inflow, $V_\infty \sin(\alpha)$
λ_m = mean inflow in momentum expression
$\bar{\lambda}_m$ = steady part of λ_m
λ_0, λ_1 = Glauert coefficients of induced flow
μ = advance ratio, $V_\infty \cos(\alpha)$
$\nu, \eta, \bar{\psi}$ = ellipsoidal coordinates, dimensionless
ξ = coordinate along freestream line, positive upstream
ρ = air density, kg/m^3
$(\rho_n^m)^2$ = integral (0 to 1) of $[P_n^m(\nu)]^2$, Eq. (14)
τ_n^{mc}, τ_n^{ms} = cosine and sine part of pressure expansion coefficients, corresponding to α_j^r and β_j^r pair
$\tilde{\tau}_n^{mc}, \tilde{\tau}_n^{ms}$ = cosine and sine part of pressure expansion coefficients, corresponding to $\tilde{\alpha}_j^r$ and $\tilde{\beta}_j^r$ pair
Φ = pressure function, dimensionless on $\rho\Omega^2R^2$
$\phi_j^r(\bar{r})$ = radial expansion shape function $\phi_j^r(\bar{r}) \equiv (1/\nu)\bar{P}_j^r(\nu)$
$\tilde{\phi}_j^r(\bar{r})$ = $\phi_j^r(\bar{r})\sqrt{\pi/(4H_n^m)}$
χ = wake skew angle, $\pi/2 - \alpha_c$
$\Psi_j^r(\bar{r})$ = general expansion functions
ψ = azimuthal location of reference blade
ψ_q = azimuth of qth blade, $\bar{t} + (2\pi/Q)(q-1)$
Ω = rotor rotational speed, rad/s
$\bar{\omega}$ = oscillation frequency, nondimensionalized on Ω

Superscript

$*$ = derivative with respect to nondimensional time, $\partial/\partial\bar{t}$

Introduction

Background

ALTHOUGH there are a great number of research tools that have increased our understanding of unsteady rotor aerodynamics, there are only a very few unsteady aerodynamic theories that can be applied to realistic problems of rotor dynamics and aeroelasticity. For lift and induced flow theories to be viable in an aeroelastic analysis, the algorithms that describe the inflow must be representable in terms of a limited number of explicit state variables. The use of explicit states is needed so that we may obtain perturbation equations in order to do Floquet theory and do control system design. Historic wake models, however, are usually not in state variable form. The most well-known methods would certainly be prescribed-wake lifting-line theories,[1] and lifting surface theories,[2] as well as free-wake lifting-line theories.[3] However, when we come to the question of performing an aeroelastic analysis of a realistic rotor, we find that such vortex-filament theories are not presently a viable alternative. First of all, for any problem beyond rigid-blade flapping, the computational effort of tracking the unsteady vorticity and of computing induced-flow integrals over hundreds of filaments at every time step is simply too large to handle on a routine basis. Second, these vortex theories are restricted to time-marching problems. They are not in a format that would allow eigenvalue analysis. Even Floquet solutions, which entail time-marching over one period for each state-variable perturbation, cannot be applied (either because the states of the flowfield are not defined explicitly or because there are too many states for realistic Floquet analysis). One can impose restrictions that allow a closed-form version of vortex theories. Such restrictions include a cylindrical wake and an infinite number of blades. Several authors have developed such theories,[4-6] but the assumption of an infinite number of blades restricts the results to only the first or second harmonic of time-averaged induced flow.

Acceleration potential theory offers an alternative tool for our understanding of rotorcraft aerodynamics. In the acceleration potential approach, one takes advantage of the fact that there is no pressure discontinuity off the lifting surface. Thus, it is possible to determine the induced flowfield with less computational effort. Also, since the acceleration potential is directly related to the blade pressure, it facilitates the formulation of the unsteady rotor wake in a form favorable to blade aeroelasticity modeling. The key ingredient in this approach is to obtain the perturbation velocity field as a function of the pressure on the blade.

It is probable that Mangler[7] was the first to apply acceleration potential theory to the computation of rotor induced flow. In his approach, the rotor is assumed to be an actuator disc with a pressure discontinuity across it. The rotor loading distribution is expanded in a series of Legendre functions that are components of the general solution to the governing equations of the acceleration potential associated with the rotor disc. The time-averaged induced velocity due to three types of axial-symmetric loading is obtained. Van Holten[8] proposed a method for calculating unsteady three-dimensional incompressible airloads on a helicopter rotor blade in steady forward flight. The method uses the acceleration potential formulation, together with a matched asymptotic expansion technique. Runyan and Tai[9] also used an acceleration potential approach to compute unsteady compressible flow around a helicopter rotor in forward flight. They modeled the lifting surface and solved the resulting integral equation by a doublet lattice approximation. All of these studies are classical fundamental formulations of unsteady aerodynamics. Thus, they do not yield explicit wake dynamics appropriate for eigenvalue analysis of the rotor system. (There are hidden states in these formulations.) Moreover, such formulations preclude efficient iterative system design due to their computational intensity.

Present Approach

As outlined in the previous review, although many methods exist for study of the unsteady wake of lifting rotors, each of these has certain drawbacks when one attemps to apply them to the analysis of rotor aeroelasticity. Somewhere between the simplest momentum and the most complicated free-wake methodologies should be an intermediate-level wake model applicable for problems of aeroelastic stability (frequency, damping, and modal information), for basic blade-passage vibrations (in the absence of signficant blade-vortex interaction), for higher-harmonic control studies, and for problems of tilt-rotor or stop-wing transitional dynamics.

Recently, the authors have developed a finite state unsteady induced-flow theory appropriate to rotorcraft aeroelasticity studies in both hover and forward flight.[10] Since then, other papers have appeared that provide closed-form expressions for the theory coefficients,[11] that extend the theory to nonlinearities associated with hover,[12] that correlate inflow with measurements,[12,13] and that correlate rotor eigenvalues with measurements.[14] Thus, since the theory has significantly evolved since 1989, and since much of the documentation is not in archival publications, the purpose of this article is to 1) document in one publication the theoretical basis of the work, 2) summarize the sundry validation efforts that are now completed, and 3) detail the theoretical and numerical applications (and limitations) of this finite state inflow theory.

Formulation

Fluid Mechanics

The basic fluid mechanics equations for an incompressible potential flow with small perturbations can be written non-

dimensionally in index notation as

$$q_{i,i} = 0 \tag{1}$$

$$\overset{*}{q}_i - V_\infty q_{i,\xi} = -\Phi_{,i} \tag{2}$$

The first equation is for conservation of mass (i.e., the continuity equation), and the second is the three components of force-momentum balance. In these equations, the q_i are the perturbation velocity components, Φ is the pressure, $(\,)^*$ is a nondimensional time derivative, $(\,)_{,\xi}$ is the derivative along the freestream line, and a repeated index implies summation. Here, we take the streamline ξ at an angle χ from the normal to the rotor disk.

As observed from Eq. (2), the spatial variation of the pressure is the superposition of contributions from both the gradient of velocity along the freestream direction (convection) and the local unsteadiness of the flowfield. This suggests a division of the pressure into two parts (i.e., the part due to convection, denoted as Φ^V, and the part due to unsteadiness denoted as Φ^A). Then, the pressure can be expressed as

$$\Phi = \Phi^V + \Phi^A \tag{3}$$

or

$$\Phi_{,i} = \Phi^V_{,i} + \Phi^A_{,i} \tag{4}$$

where

$$\Phi^V_{,i} = V_\infty q_{i,\xi} \tag{5}$$

$$\Phi^A_{,i} = -\overset{*}{q}_i \tag{6}$$

If we differentiate Eq. (2) with respect to the index i, with the help of continuity Eq. (1), a Laplace's equation for the pressure function can be obtained as follows:

$$\Phi_{,ii} = 0 \tag{7}$$

In a similar way, from Eqs. (4) and (5), we have

$$\Phi^V_{,ii} = 0 \tag{8}$$

$$\Phi^A_{,ii} = 0 \tag{9}$$

Equations (8) and (9) indicate that each part of the total pressure satisfies Laplace's equation, which is significant for the formulation of the theory. The boundary conditions for each Φ component are that the pressure matches the known blade loading on the rotor blades (which are assumed to always lie on a circular disk), and to be zero at infinity (the condition of zero perturbation pressure at infinity is not exactly true inside of the rotor wake, but this is neglected in this theory).

When written in ellipsoidal coordinates (see the Appendix, Fig. A1), Laplace's Eq. (7) associated with a circular disk can be solved analytically by the method of separation of variables. The potential functions thus obtained give an arbitrary pressure discontinuity across the disk due to the equivalent of acceleration doublets. Application of the zero-pressure perturbation condition at infinity yields a suitable general solution for the acceleration potential

$$\Phi(\nu, \eta, \bar{\psi}, \bar{t}) = \sum_{m=0}^{\infty} \sum_{n=m+1,m+3,\ldots}^{\infty} P_n^m(\nu) Q_n^m(i\eta) \times [C_n^m(\bar{t})\cos(m\bar{\psi}) + D_n^m(\bar{t})\sin(m\bar{\psi})] \tag{10}$$

where $P_n^m(\nu)$ and $Q_n^m(i\eta)$ are associated Legendre functions of the first and second kind, respectively; C_n^m and D_n^m are arbitrary coefficients to be determined; and ν, η, and $\bar{\psi}$ are ellipsoidal coordinates as described in Appendix A. In the summation [Eq. (10)], only those terms with $n + m$ odd are retained, because $P_n^m(\nu)$ with $n + m$ even do not match the boundary condition of zero pressure at the edge of the disk. Terms of the type $P(i\nu)$ and $Q(\eta)$ are rejected because they do not give zero pressure at infinity. Also, in Eq. (10), the Legendre function $P_n^m(\nu)$ is defined only for $n \geq m$.

Equation (10) is related to the solutions for circular wings found in the literature.[15-17] However, here we have no nonpenetration boundary condition or Kutta condition. Furthermore, the pressure must be zero at the rotor edge. Thus, the extra singular potential solutions are not required. Also, the unsteady solution in Ref. 16 is treated in the frequency domain (as in Theodorsen theory), whereas here we develop a finite state solution.

It is important to note that, since ν is positive above the disk and negative below the disk, the pressure function Φ with $n + m$ odd yields a discontinuity in pressure across the disk where $\eta = 0$, $\nu = \sqrt{1 - \bar{r}^2}$, and $\bar{\psi} = \psi$. Therefore, rotor lift can be expressed as the pressure difference between the upper and the lower surfaces of the disk

$$P(\bar{r}, \psi, \bar{t}) = -2 \sum_{m=0}^{\infty} \sum_{n=m+1,m+3,\ldots}^{\infty} P_n^m(\nu) Q_n^m(i0) \times [C_n^m(\bar{t})\cos(m\psi) + D_n^m(\bar{t})\sin(m\psi)] \tag{11}$$

or

$$P(\bar{r}, \psi, \bar{t}) = \sum_{m=0}^{\infty} \sum_{n=m+1,m+3,\ldots}^{\infty} \bar{P}_n^m(\nu)[\tau_n^{mc}(\bar{t})\cos(m\psi) + \tau_n^{ms}(\bar{t})\sin(m\psi)] \tag{12}$$

where

$$\bar{P}_n^m(\nu) = (-1)^m [P_n^m(\nu)/\rho_n^m] \tag{13}$$

$$(\rho_n^m)^2 = \frac{1}{2n+1} \frac{(n+m)!}{(n-m)!} \tag{14}$$

$$\tau_n^{mc} = (-1)^{m+1} 2 Q_n^m(i0) \rho_n^m C_n^m \tag{15}$$

$$\tau_n^{ms} = (-1)^{m+1} 2 Q_n^m(i0) \rho_n^m D_n^m \tag{16}$$

The $\bar{P}_n^m(\nu)$ are so defined for mathematical conditioning, and they may be called normalized associated Legendre functions of the first kind since they result in

$$\int_0^1 [\bar{P}_n^m(\nu)]^2 \, d\nu = 1, \qquad \bar{P}_{m+1}^m(\nu) > 0 \tag{17}$$

It is also helpful to use the normalized variables τ_n^{mc}, and τ_n^{ms} in the global pressure

$$\Phi = -\frac{1}{2} \sum_{m=0}^{\infty} \sum_{n=m+1,m+3,\ldots}^{\infty} \bar{P}_n^m(\nu) \bar{Q}_n^m(i\eta) \times [\tau_n^{mc}(\bar{t})\cos(m\bar{\psi}) + \tau_n^{ms}(\bar{t})\sin(m\bar{\psi})] \tag{18}$$

where we have introduced

$$\bar{Q}_n^m(i\eta) \equiv [Q_n^m(i\eta)/Q_n^m(i0)] \tag{19}$$

Since both Φ^V and Φ^A satisfy Laplace's equation, Eq. (18) can be utilized to represent each of them:

$$\Phi^V = -\frac{1}{2}\sum_{m=0}^{\infty}\sum_{n=m+1,m+3,\ldots}^{\infty}\bar{P}_n^m(\nu)\bar{Q}_n^m(i\eta) \times [(\tau_n^{mc})^V\cos(m\bar{\psi}) + (\tau_n^{ms})^V\sin(m\bar{\psi})] \tag{20}$$

$$\Phi^A = -\frac{1}{2}\sum_{m=0}^{\infty}\sum_{n=m+1,m+3,\ldots}^{\infty}\bar{P}_n^m(\nu)\bar{Q}_n^m(i\eta) \times [(\tau_n^{mc})^A\cos(m\bar{\psi}) + (\tau_n^{ms})^A\sin(m\bar{\psi})] \tag{21}$$

To establish a relation between the induced flow of a lifting rotor and the blade loads, let us start with Eqs. (5) and (6). Integration of Eq. (5) along the freestream direction results in a relationship between velocity and Φ^V

$$q_i = -\frac{1}{V_\infty}\int_\xi^\infty \Phi_{,i}^V\,d\xi \tag{22}$$

where the ∞ cannot be inside the rotor wake due to the boundary condition $q_i(\infty) = 0$. A relationship between velocity and Φ^A can be obtained from Eq. (6):

$$\overset{*}{q}_i = -\Phi_{,i}^A \tag{23}$$

Now, if we are only interested in the z component of the perturbation velocity at $\xi = 0$ (i.e., the normal component of induced inflow at the rotor disk), Eqs. (22) and (23) can be placed in the following forms:

$$w = -\frac{1}{V_\infty}\int_0^\infty \frac{\partial\Phi^V}{\partial z}\,d\xi \tag{24}$$

$$\overset{*}{w} = -\frac{\partial\Phi^A}{\partial z}\bigg|_{\eta=0} \tag{25}$$

Equations (24) and (25) can be thought of as linear operations on Φ to obtain w:

$$w = L[\Phi^V] \tag{26}$$

$$\overset{*}{w} = E[\Phi^A] \tag{27}$$

At this stage, we assume that the operators L and E are invertible. Then, we can write a time-domain induced-flow theory based on Eq. (3) in the following form:

$$E^{-1}[w]^* + L^{-1}[w] = \Phi^A + \Phi^V = \Phi \tag{28}$$

Therefore, if we can find these inverse operators, then we can formulate the induced-flow theory for rotors. As will be seen immediately, with a proper series expansion for induced flow, both operators L and E can be expressed in a matrix form, and thus, can be inverted by methods of linear algebra.

The induced flow distribution can be represented in an analogous expansion to that used for pressure in terms of a harmonic variation in azimuth and arbitrary radial distribution functions Ψ_j^r

$$w(\bar{r},\psi,\bar{t}) = \sum_{r=0}^{\infty}\sum_{j=r+1,r+3,\ldots}^{\infty}\Psi_j^r(\bar{r})[a_j^r(\bar{t})\cos(r\psi) + b_j^r(\bar{t})\sin(r\psi)] \tag{29}$$

where the set of radial expansion functions, the $\Psi_j^r(\bar{r})$, must be linearly independent and complete (within the constraints at $\bar{r} = 0$) for a given harmonic r. The a_j^r and b_j^r are induced flow expansion coefficients and can be regarded as the time-dependent states of the induced-flow model. One obvious choice for $\Psi_j^r(\bar{r})$ is the set of normalized Legendre functions used in the pressure representation

$$w(\bar{r},\psi,\bar{t}) = \sum_{r=0}^{\infty}\sum_{j=r+1,r+3,\ldots}^{\infty}\bar{P}_j^r(\nu)[c_j^r(\bar{t})\cos(r\psi) + d_j^r(\bar{t})\sin(r\psi)] \tag{30}$$

where the c_j^r and d_j^r are induced flow states related to the $\bar{P}_j^r(\nu)$ expansion. However, this choice does have the disadvantage that

$$\bar{P}_j^r(\bar{r})\big|_{\bar{r}=1} = \bar{P}_j^r(\nu)\big|_{\nu=0} = 0 \tag{31}$$

which could imply slow convergence of velocity near the blade tip. Therefore, we consider an alternate choice to overcome this barrier:

$$\Psi_j^r(\bar{r}) = \phi_j^r(\bar{r}) \equiv (1/\nu)\bar{P}_j^r(\nu) \tag{32}$$

then

$$w(\bar{r},\psi,\bar{t}) = \sum_{r=0}^{\infty}\sum_{j=r+1,r+3,\ldots}^{\infty}\phi_j^r(\bar{r})[\alpha_j^r(\bar{t})\cos(r\psi) + \beta_j^r(\bar{t})\sin(r\psi)] \tag{33}$$

The radial expansion functions $\phi_j^r(\bar{r})$ have the following form:

$$\phi_j^r(\bar{r}) = \sqrt{(2j+1)H_j^r}\sum_{q=r,r+2,\ldots}^{j-1}\times \bar{r}^q\frac{(-1)^{(q-r)/2}(j+q)!!}{(q-r)!!(q+r)!!(j-q-1)!!} \tag{34}$$

where

$$H_j^r = \frac{(j+r-1)!!(j-r-1)!!}{(j+r)!!(j-r)!!} \tag{35}$$

Interestingly enough, the $\phi_j^r(\bar{r}) \equiv (1/\nu)\bar{P}_j^r(\nu)$ are simply polynomials in the radial position $\bar{r}$, having only even (or odd) powers ranging from $(\bar{r})^r$ to $(\bar{r})^{j-1}$ ($j + r$ is odd, and $j > r$).

With pressure and velocity each represented by the above expansions with like number of terms, the operators in Eq. (28) can be expressed as square matrices that relate the pressure coefficients (τ_n^{mc}, τ_n^{ms}) to the velocity coefficients (α_j^r, β_j^r). Thus, Eq. (28), multiplied by a factor of 2, becomes

$$[M]\begin{Bmatrix}\vdots\\ \{\alpha_j^r\}\\ \vdots\end{Bmatrix}^* + [L^c]^{-1}\begin{Bmatrix}\vdots\\ \{\alpha_j^r\}\\ \vdots\end{Bmatrix} = \begin{Bmatrix}\vdots\\ \{\tau_n^{mc}\}\\ \vdots\end{Bmatrix} \tag{36}$$

$$[M]\begin{Bmatrix}\vdots\\ \{\beta_j^r\}\\ \vdots\end{Bmatrix}^* + [L^s]^{-1}\begin{Bmatrix}\vdots\\ \{\beta_j^r\}\\ \vdots\end{Bmatrix} = \begin{Bmatrix}\vdots\\ \{\tau_n^{ms}\}\\ \vdots\end{Bmatrix} \tag{37}$$

where $[M]$ represents the inverse of the E operator; and $[L^c]$, $[L^s]$ are the L operators for cosine and sine components, respectively.

Matrix Operators

The first term in each of Eqs. (36) and (37) is related to the unsteadiness of pressure. It comes from the E operator that is associated with the acceleration part of the induced flow. Thus, it can well be called an apparent mass matrix. It turns out that the simplest form of this mass-matrix operator relates to the $\phi_n^m(\bar{r})$ expansion, Eq. (33). The computation of the M matrix involves implementation of the operation in Eq. (25). First of all, according to the transformation from the

rotor disk coordinates to ellipsoidal coordinates, as described in the Appendix, application of the chain rule yields

$$\frac{\partial}{\partial z} = -\frac{1}{\nu^2 + \eta^2}\left[\eta(1 - \nu^2)\frac{\partial}{\partial \nu} + \nu(1 + \eta^2)\frac{\partial}{\partial \eta}\right] \quad (38)$$

At the rotor disk, $\eta = 0$, this equation reduces to a simple form:

$$\frac{\partial}{\partial z} = -\frac{1}{\nu}\frac{\partial}{\partial \eta} \quad (39)$$

Substitution of Eqs. (21), (33), and (39) into Eq. (25), and with the help of orthogonality of both associated Legendre functions of the first kind and trigonometric functions, we obtain

$$\alpha_n^{*m} = -\left.\frac{d\bar{Q}_n^m(i\eta)}{d\eta}\right|_{\eta=0}\frac{1}{2}(\tau_n^{mc})^A \quad (40)$$

$$\beta_n^{*m} = -\left.\frac{d\bar{Q}_n^m(i\eta)}{d\eta}\right|_{\eta=0}\frac{1}{2}(\tau_n^{ms})^A \quad (41)$$

where

$$-\left.\frac{d\bar{Q}_n^m(i\eta)}{d\eta}\right|_{\eta=0} = \frac{\pi}{2}(H_n^m)^{-1} \quad (42)$$

$$H_n^m = \frac{(n + m - 1)!!(n - m - 1)!!}{(n + m)!!(n - m)!!} \quad (43)$$

Therefore, the $[M]$ matrix is a diagonal made up of terms $(4H_n^m/\pi)$. For application, it is advantageous to have $[M] = I$. Therefore, we take the w expansion in Eq. (33) to be in terms of polynomials normalized on $2\sqrt{H_j^r/\pi}$:

$$\tilde{\phi}_j^r(\bar{r}) = \frac{1}{2}\sqrt{\pi(2j + 1)} \times \sum_{q=r,r+2,\ldots}^{j-1} \bar{r}^q \frac{(-1)^{(q-r)/2}(j + q)!!}{(q - r)!!(q + r)!!(j - q - 1)!!} \quad (44)$$

Thus,

$$w(\bar{r}, \psi, \bar{t}) = \sum_{r=0}^{\infty}\sum_{j=r+1,r+3,\ldots}^{\infty}\tilde{\phi}_j^r(\bar{r}) \times [\tilde{\alpha}_j^r(\bar{t})\cos(r\psi) + \tilde{\beta}_j^r(\bar{t})\sin(r\psi)] \quad (45)$$

Then, we divide each row in Eqs. (36) and (37) by $2\sqrt{H_j^r/\pi}$ to give $[M] = I$ for both sine and cosine equations.

The $[L]$ matrix (or operator) takes on two different forms: one for cosine $[L^c]$, and one for sine $[L^s]$. To compute this matrix, it is most convenient to use the $\bar{P}_n^m(\nu)$ expansion, Eq. (30). We substitute Eqs. (20) and (30) into Eq. (24), multiply by $\bar{P}_j^r(\nu_0)\cos(r\psi)$ or $\bar{P}_j^r(\nu_0)\sin(r\psi)$, where ν_0 and ψ are the ν and ψ on the disk from which the streamline emanates; and we integrate both radially and azimuthally. By taking advantage of the orthogonality, of both associated Legendre functions $\bar{P}_n^m(\nu)$ in the interval $[0, 1]$ and of trigonometric functions in $[0, 2\pi]$, we obtain linear relations between inflow states and pressure of the form

$$\begin{Bmatrix}\vdots\\ \{\alpha_j^r\}\\ \vdots\end{Bmatrix} = \frac{1}{V_\infty}\begin{bmatrix}\cdots & \vdots & \cdots\\ & [\hat{L}_{jn}^{rm}]^c & \\ & \vdots & \end{bmatrix}\begin{Bmatrix}\vdots\\ \{(\tau_n^{mc})^V\}\\ \vdots\end{Bmatrix} \quad (46)$$

$$\begin{Bmatrix}\vdots\\ \{\beta_j^r\}\\ \vdots\end{Bmatrix} = \frac{1}{V_\infty}\begin{bmatrix}\cdots & \vdots & \cdots\\ & [\hat{L}_{jn}^{rm}]^s & \\ & \vdots & \end{bmatrix}\begin{Bmatrix}\vdots\\ \{(\tau_n^{ms})^V\}\\ \vdots\end{Bmatrix} \quad (47)$$

The elements of $\hat{L}$ are computed from the following expressions:

$$\hat{L}_{jn}^{0mc} = \frac{1}{4\pi}\int_0^{2\pi}\int_0^1 \bar{P}_j^0(\nu_0)\int_0^\infty \frac{\partial}{\partial z}[\bar{P}_n^m(\nu)\bar{Q}_n^m(i\eta)] \times \cos(m\bar{\psi})\, d\xi\, d\nu_0\, d\psi \quad (48)$$

$$\hat{L}_{jn}^{rmc} = \frac{1}{2\pi}\int_0^{2\pi}\int_0^1 \bar{P}_j^r(\nu_0)\cos(r\psi)\int_0^\infty \frac{\partial}{\partial z}[\bar{P}_n^m(\nu)\bar{Q}_n^m(i\eta)] \times \cos(m\bar{\psi})\, d\xi\, d\nu_0\, d\psi \quad (49)$$

$$\hat{L}_{jn}^{rms} = \frac{1}{2\pi}\int_0^{2\pi}\int_0^1 \bar{P}_j^r(\nu_0)\sin(r\psi)\int_0^\infty \frac{\partial}{\partial z}[\bar{P}_n^m(\nu)\bar{Q}_n^m(i\eta)] \times \sin(m\bar{\psi})\, d\xi\, d\nu_0\, d\psi \quad (50)$$

where ξ emanates at an angle of χ away from the z axis.

The circumflex indicates that $\hat{L}$ is for the special case of the $\bar{P}_n^m(\nu)$ expansion with V_∞ factored out. The $\hat{L}$ is partitioned such that the superscripts are row-column indices of the r-m partition, and the subscripts (j, n) are the row-column indices of the elements within each partition. We must note, however, that these indices do not take the traditional matrix values of 1, 2, 3, ... Instead, for the cosine equation, we have $m = 0, 1, 2, 3, \ldots$, and $r = 0, 1, 2, 3, \ldots$; for the sine equation, $m = 1, 2, 3, \ldots$, and $r = 1, 2, 3, \ldots$; and, for either set, $j = r + 1, r + 3, r + 5, \ldots$ or $n = m + 1, m + 3, m + 5, \ldots$. Interestingly, for axial flow, $\chi = 0$, $(\xi = -z)$, $\hat{L}$ reduces to the identity matrix for both sine and cosine, as will be shown later.

Although, the integrals in Eqs. (48), (49), and (50) may seem hopelessly complex, they have been worked out in closed form, and the formulas have been verified through comparisons with numerical evaluation of the integrals. The elements of $\hat{L}$ depend only on the wake skew angle χ ($\chi = 0$ in axial flow, $\chi = 90$ deg in edgewise flow).[18] After we transform to a $\tilde{\phi}_j^r$ series $(\tilde{\alpha}_j^r, \tilde{\beta}_j^r)$, and divide each equation by $\sqrt{H_n^m/\pi}$, $\hat{L}$ becomes L:

$$[\tilde{L}_{jn}^{0m}]^c = (X^m)[\Gamma_{jn}^{0m}] \quad (51)$$

$$[\tilde{L}_{jn}^{rm}]^c = [X^{|m-r|} + (-1)^l X^{|m+r|}][\Gamma_{jn}^{rm}] \quad (52)$$

$$[\tilde{L}_{jn}^{rm}]^s = [X^{|m-r|} - (-1)^l X^{|m+r|}][\Gamma_{jn}^{rm}] \quad (53)$$

where $l = \min(r, m)$, and $X = \tan|\chi/2|$. Note that $0 \le X \le 1$.

All sine and cosine elements rely on the same coefficients Γ_{jn}^{rm} that can be expressed in closed-form as follows:

for $r + m$ even

$$\Gamma_{jn}^{rm} = \frac{(-1)^{(n+j-2r)/2}4\sqrt{(2n + 1)(2j + 1)}}{\pi(j + n)(j + n + 2)[(j - n)^2 - 1]} \quad (54)$$

for $r + m$ odd, $j = n \pm 1$

$$\Gamma_{jn}^{rm} = \frac{\text{sgn}(r - m)}{\sqrt{(2n + 1)(2j + 1)}} \quad (55)$$

for $r + m$ odd, $j \neq n \pm 1$

$$\Gamma_{jn}^{rm} = 0 \quad (56)$$

This is the most compact form of the theory.

As a further refinement of the perburbation theory, the V_∞ in Eqs. (46) and (47) can be replaced with an equivalent V to account for the influence of induced flow on the total steady

flow through the rotor disk. A complete derivation is given in Ref. 19. The resultant V is

$$V = [\mu^2 + (\lambda + \bar{\lambda}_m)\lambda/\sqrt{\mu^2 + \lambda^2}] \tag{57}$$

$$\lambda = \bar{\lambda}_m + \lambda_f \tag{58}$$

The $\bar{\lambda}_m$ is the momentum-theory value of steady induced flow for a trimmed rotor

$$\bar{\lambda}_m = \tfrac{1}{2}(\bar{C}_T/V_T) \cong (\sqrt{3\pi}/2)\bar{\alpha}_1^0 \tag{59}$$

where $\bar{C}_T$ is steady thrust, $\bar{\alpha}_1^0$ is the steady uniform induced flow, and $V_T = \sqrt{\mu^2 + \lambda^2}$. Our wake model can then be considered as a theory for perturbation pressure and velocity about this steady condition. In axial flight ($\mu = 0$), the mass-flow parameter reduces to

$$\begin{aligned} V &= \lambda + \bar{\lambda}_m \\ &= \lambda_f + 2\bar{\lambda}_m \end{aligned} \tag{60}$$

which is the same as momentum theory.

Furthermore, in application of the wake theory, α_c should be taken as $\chi = (\pi/2) - \alpha_c$. This modification accounts for the influence of inflow perturbation on global wake skewing in an averaged manner, and cannot be ignored. Thus, we use

$$\alpha_c = \tan^{-1}|\lambda/\mu| \tag{61}$$

$$\chi = \tan^{-1}|\mu/\lambda| \tag{62}$$

The above extends the theory from one linearized about freestream V_∞, to one linearized about the momentum theory value of $\bar{\alpha}_1^0$. This is accurate because the first element of the $\bar{L}^c$ matrix $\bar{L}_{11}^{00}$, is independent of wake skew angle. As a final generalization, the theory can be integrated to obtain one that is nonlinear in $\bar{\alpha}_1^0$, although linear in all other $\bar{\alpha}_n^m$, $\bar{\beta}_n^m$. Reference 19 shows that this is very accurate in hover. (The nonlinearity has little effect on forward flight for which V is dominated by μ.) The resultant nonlinear equations are

$$\begin{Bmatrix} \vdots \\ \bar{\alpha}_n^m \\ \vdots \end{Bmatrix}^* + [\bar{L}^c]^{-1} \begin{bmatrix} \ddots & & \\ & V_n^m & \\ & & \ddots \end{bmatrix} \begin{Bmatrix} \vdots \\ \bar{\alpha}_n^m \\ \vdots \end{Bmatrix} = \begin{Bmatrix} \vdots \\ \bar{\tau}_n^{mc} \\ \vdots \end{Bmatrix} \tag{63}$$

$$\begin{Bmatrix} \vdots \\ \bar{\beta}_n^m \\ \vdots \end{Bmatrix}^* + [\bar{L}^s]^{-1} \begin{bmatrix} \ddots & & \\ & V_n^m & \\ & & \ddots \end{bmatrix} \begin{Bmatrix} \vdots \\ \bar{\beta}_n^m \\ \vdots \end{Bmatrix} = \begin{Bmatrix} \vdots \\ \bar{\tau}_n^{ms} \\ \vdots \end{Bmatrix} \tag{64}$$

where $\bar{\lambda}_m$ is replaced by λ_m in V, and V_T and

$$V_1^0 = V_T \tag{65}$$

$$V_n^m = V \quad \text{for} \quad n, m \neq 1, 0 \tag{66}$$

with

$$\lambda_m = (\sqrt{3\pi}/2)\bar{\alpha}_1^0 \tag{67}$$

which is in terms of the instantaneous value of $\bar{\alpha}_1^0$. Thus, nonlinearities of the form $\bar{\alpha}_1^0\bar{\alpha}_n^m$ appear in the equations. Reference 18 shows that a perturbation of Eqs. (63) and (64) recovers the original equations if the wake skew angle is fixed and if the static solution has uniform inflow $\bar{\alpha}_1^0$.

Limitations

It should be pointed out that there are several crucial limitations to the above approach. First, the rotor is assumed to consist of acceleration doublets that remain in a thin, undeformed disk. Thus, effects of dihedral or blade out-of-plane bending on the wake are not included. Second, all loads are considered to be normal to this disk. Thus, induced flow due to inplane lift is not considered. Third, this model implies a skewed, cylindrical wake. Thus, effects of wake distortion and roll-up are neglected. Fourth, the singular potential functions are not included. Thus, the theory cannot converge to a circular wing nor compute lift due to radial flow along a blade (although it does converge to an actuator disk with zero pressure at the edges). Therefore, one should not infer that this model can replace vortex-lattice models for all applications. Its primary utility is that it provides a state-space model that can be used in aeroelasticity and control applications.

Application

Generalized Forces

The pressure coefficients τ_n^{mc} and τ_n^{ms} in Eqs. (36) and (37) serve as the inflow generalized forces, or the inflow forcing functions, and offer the interface between the wake and lift models. In order to be coupled with blade lift theory, the τ_n^{mc} and τ_n^{ms} need to be appropriately related to the blade circulatory lift. To do this, we assume a rotor with a finite number of blades so that the rotor disk loading is discontinuously distributed at the instantaneous position of each rotor blade. This is to say that the air loading is finite only on the blade planform, and zero elsewhere. Suppose that the lift is available at every instant time $\bar{t}$. We then would have the pressure on the qth blade written as $P_q(\bar{r}, \bar{y}, \bar{t})$, where $\bar{y}$, is defined from $-\bar{b}$ to $+\bar{b}$ across the blade chord for which $\psi = \psi_q + \sin^{-1}(\bar{y}/\bar{r})$; and pressure is zero elsewhere. Then, we can expand this discontinuous distribution in terms of Legendre functions:

$$\begin{aligned} P_q(\bar{r}, \omega, \bar{t}) = \sum_{m=0}^{\infty} \sum_{n=m+1, m+3, \ldots}^{\infty} \bar{P}_n^m(\nu)[&\tau_n^{mc}(\bar{t})\cos(m\psi) \\ &+ \tau_n^{ms}(\bar{t})\sin(m\psi)] \end{aligned} \tag{68}$$

Accordingly, the τ_n^{mc} and τ_n^{ms} can be obtained as

$$\tau_n^{0c} = \frac{1}{2\pi} \sum_{q=1}^{Q} \int_0^1 \int_{-\bar{b}}^{\bar{b}} P_q(\bar{r}, \bar{y}, \bar{t})\phi_n^0(\bar{r})\, d\bar{r}\, d\bar{y} \tag{69}$$

$$\tau_n^{mc} = \frac{1}{\pi} \sum_{q=1}^{Q} \int_0^1 \int_{-\bar{b}}^{\bar{b}} P_q(\bar{r}, \bar{y}, \bar{t})\phi_n^m(\bar{r})\cos(m\psi)\, d\bar{r}\, d\bar{y} \tag{70}$$

$$\tau_n^{ms} = \frac{1}{\pi} \sum_{q=1}^{Q} \int_0^1 \int_{-\bar{b}}^{\bar{b}} P_q(\bar{r}, \bar{y}, \bar{t})\phi_n^m(\bar{r})\sin(m\psi)\, d\bar{r}\, d\bar{y} \tag{71}$$

where $\bar{y}$ is nondimensional chordwise coordinate with its origin at midchord, and ψ is azimuth angle as in Fig. 1. It is also noted that $d\nu\, d\psi$ has been expressed in terms of $d\bar{r}\, d\bar{y}$ on each blade (at ψ_q), and $\phi_n^m = (1/\nu)\bar{P}_n^m(\nu)$ is used. If a

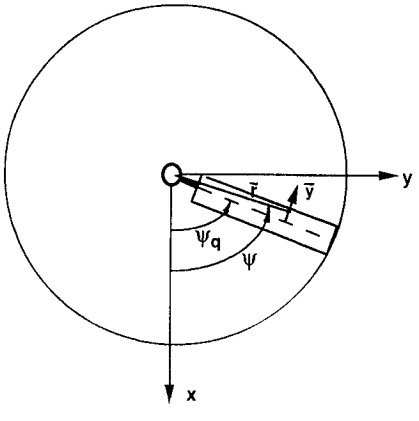

Fig. 1 Evaluation of inflow forcing functions.

particular blade theory does not provide chordwise pressure, we may assume a chordwise distribution $P_{\bar{y}}(\bar{y})$, such that

$$P_q(\bar{r}, \bar{y}, \bar{t}) = \bar{L}_q(\bar{r}, \bar{t}) P_{\bar{y}}(\bar{y}) \Big/ \int_{-\bar{b}}^{\bar{b}} P_{\bar{y}}(\bar{y})\, d\bar{y} \tag{72}$$

After substitution of Eq. (72) into Eqs. (69–71), we can perform the chordwise integral for the τ_n^m equations.

From the above results, the final τ_n^m equations, for small $\bar{b}/\bar{r}$, can be written in a concise complex form

$$\begin{aligned} \tau_n^{me} &\equiv \tfrac{1}{2}(\tau_n^{mc} - i\tau_n^{ms}) \\ &= \frac{1}{2\pi} \sum_{q=1}^{Q} \left[\int_0^1 f_m \bar{L}_q \phi_n^m(\bar{r})\, d\bar{r} \right] e^{-im\psi_q} \end{aligned} \tag{73}$$

where the function f_m represents the integral of chordwise pressure distribution, and is given by

$$f_m(m\bar{b}/\bar{r}) = \frac{\int_{-\bar{b}}^{\bar{b}} P\bar{y}(\bar{y}) e^{(-im\bar{y}/\bar{r})}\, d\bar{y}}{\int_{-\bar{b}}^{\bar{b}} P_{\bar{y}}(\bar{y})\, d\bar{y}} \tag{74}$$

For the $\bar{\phi}_j^r$ expansion of the induced flow, Eqs. (63) and (64), the corresponding $\bar{\tau}_n^m$ integrals are

$$\begin{aligned} \bar{\tau}_n^{me} &\equiv \tfrac{1}{2}(\bar{\tau}_n^{mc} - i\bar{\tau}_n^{ms}) \\ &= \frac{1}{2\pi} \sum_{q=1}^{Q} \left[\int_0^1 f_m \bar{L}_q \bar{\phi}_n^m(\bar{r})\, d\bar{r} \right] e^{-im\psi_q} \end{aligned} \tag{75}$$

The functions f_m, which appear in the $\bar{\tau}_n^m$ equations, can be found for any given chordwise pressure distribution. From Eq. (74), it is noted that f_m is only a function of $m\bar{b}/\bar{r}(\equiv k_m)$. Figure 2 shows six different chordwise distributions and resultant values of f_m. The first three are for distributions centered about the midchord. These give $f_m = 1$ for a lifting line, $f_m = \sin(k_m)/k_m$ for a uniform pressure, and $f_m = J_0(k_m)$ for the Glauert distribution. The last three are for distributions with c.p. at the quarterchord. These give complex values (i.e., $\bar{\tau}_n^{mc}$ depends on a $\sin(m\psi_q)$ integral, and vice versa). For $(k_m)^2 \ll 1$, the first two f_m are approximately 1, and the last three are approximately $1 - ik_m/2$. All five are equal to 1 for the zero harmonic.

Strictly speaking, a theory with $f_m = 1$ for all harmonics (a lifting line at the point of velocity computation) does not converge on velocity at $\bar{y} = 0$ as the number of harmonics increases without bound. (This is to be expected, since it is well-known that unsteady lifting-line theory has a singular integral and an infinite imaginary part of the lift-deficiency function.) Nevertheless, for realistic helicopter parameters and $m < 30$, we find that $f_m = 1$ is numerically accurate. (It is well-known that some series can be very useful and accurate with a few terms, although they diverge with an infinite number of terms.[20]) Therefore, one may reasonably take $f_m = 1$ with little loss of accuracy. On the other hand, if one wishes to include more than 30 harmonics, the choice $f_m = \sin(k_m)/k_m$ or $f_m = J_0(k_m)$ converges well and effectively filters out the effect of bound vorticity from the computation.

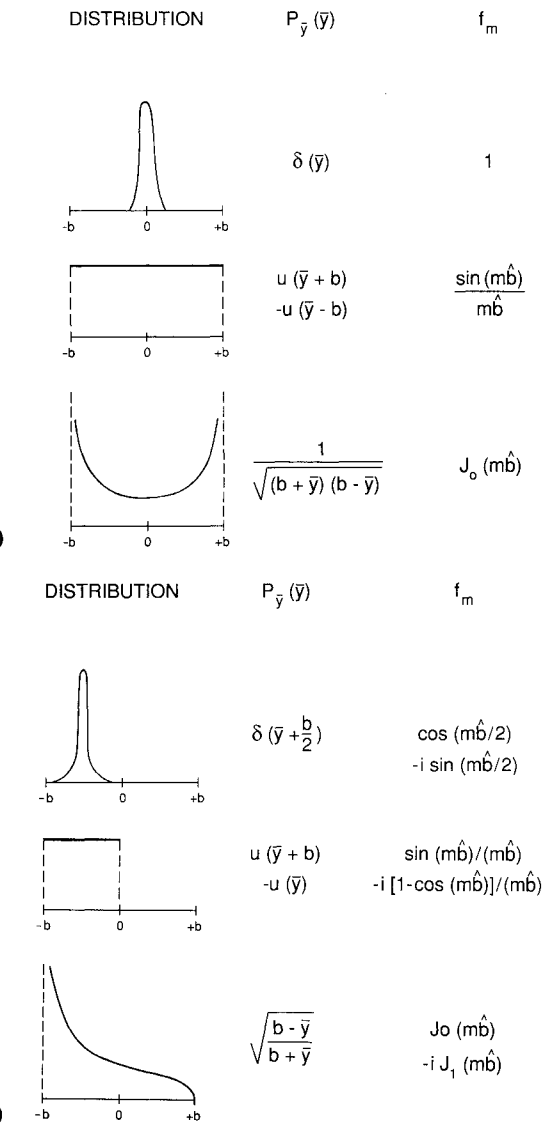

Fig. 2 Chordwise pressure distributions: a) centered about the midchord and b) c.p. at the quarterchord.

Lift Theory

For the lift $\bar{L}_q$ in Eq. (75), one could apply any theory that provides circulatory lift based on the time history of induced flow. For example, Refs. 11 and 21 utilize the ONERA dynamic stall theory. In this article, we invoke the Prandtl assumption that the sectional lift can be found from a two-dimensional analysis of the nonpenetration boundary condition, but with the induced flow in that condition coming from the three-dimensional wake model. Thus, we use the lift equations from Part I of this article. Here, we have renormalized the results on blade radius and tip speed (as opposed to semichord and local freestream, as in Part I). The resultant equations are

$$\bar{L}_y = 2\pi\bar{b}u_0(w_0 + \tfrac{1}{2}w_1 - \lambda_0) + \pi\bar{b}^2(\overset{*}{w}_0 - \tfrac{1}{2}\overset{*}{w}_2) \tag{76}$$

$$\bar{L}_q = 2\pi\bar{b}u_0(w_0 + \tfrac{1}{2}w_1 - \lambda_0 - \tfrac{1}{2}\lambda_1) \tag{77}$$

where airfoil motions and iduced flow are normalized on ΩR. The Glauert coefficients of inflow λ_n can be obtained from integration of the induced flow across the blade chord. The result is

$$\lambda_0 = \sum_{r,j}^{\infty} \bar{\phi}_j^r(\bar{r}) J_0(r\hat{b})[\bar{\alpha}_j^r \cos(r\psi_q) + \bar{\beta}_j^r \sin(r\psi_q)] \tag{78}$$

$$\lambda_1 = 2\sum_{r,j}^{\infty} \bar{\phi}_j^r(\bar{r}) J_1(r\hat{b})[\bar{\alpha}_j^r \sin(r\psi_q) - \bar{\beta}_j^r \cos(r\psi_q)] \tag{79}$$

As with the $\bar{\tau}_n^m$ integrals, most rotors are slender enough that we may take $J_0(r\hat{b}) = 1$, and $J_1(r\hat{b}) = 0$. The neglect of λ_1 has little effect for $k < 0.2$ (typical of rotors). Furthermore, for some pressure distributions, the λ_1 series is divergent or

has a steady-state error. Thus, it is suggested that λ_1 be neglected in the $\bar{\tau}_n'''$ integrals.

Although V_∞ can intersect the disc at an arbitrary angle, the moving blades see a relatively low angle of attack. Thus, the vorticity in the rotating system is shed exactly at the trailing edge (when the Glauert distribution is applied). In the nonrotating system, however, the vorticity is seen to propagate at the steeper angle of attack α_e.

Results

Because the theory has been applied extensively in the literature, there is little need for a lengthy set of results here. Instead, we present a few typical results to verify the accuracy of the theory. First, we take the two-dimensional limit of the present theory in which we neglect radial functions. Figure 3 shows results of our theory with 12 and 24 harmonics (J = 3, 6), as compared with Lowey theory both with $C(k)$ and $C(k) = 1$ (near wake). The results, from Ref. 10, are for the differential mode. Note in the region $0 < \omega_r < 1.0$, $k < 0.1$, that the present theory captures the $C(k)$ effects [primarily $k\,\mathrm{Im}(k)$] very accurately. A second comparison is given for the full three-dimensional theory in axial flow for a one-bladed rotor (Fig. 4, Ref. 12). The radial distribution of induced velocity is computed for 16 harmonics and both 1 and 4 shape functions per harmonic. Comparison with the Prandtl formula shows a good convergence for the effect of trailed vorticity. Also from Ref. 12 is a comparison with unsteady flow measurements in hover. Figure 5 shows these comparisons. Note that, since this is in hover, the full nonlinear version is exercised. Both the average and blade passage velocities are well-modeled with 24 harmonics.

Figures 6 and 7, Ref. 13, give computed and measured induced flow contours in forward flight. The computation has 8 harmonics and 33 total state variables. The correlation between measured and computed induced flow is excellent, and Ref. 13 shows the present method to be superior to conventional vortex lattice methods in accuracy. Finally, Fig. 8 shows results for the lift on a rectangular wing (stopped rotor) of aspect ratio 10, taken from Ref. 22. The plain line is the Prandtl lifting-line solution, and the open symbols are the finite state model with 8 harmonics (22 states). The agreement is excellent, and this same agreement is found at all aspect ratios from 5 to 30. Thus, the model seems to give good results, even in the limit of a stopped rotor.

It is also interesting that the present analysis includes dynamic inflow theory explicitly (as the first three states, α_1^0,

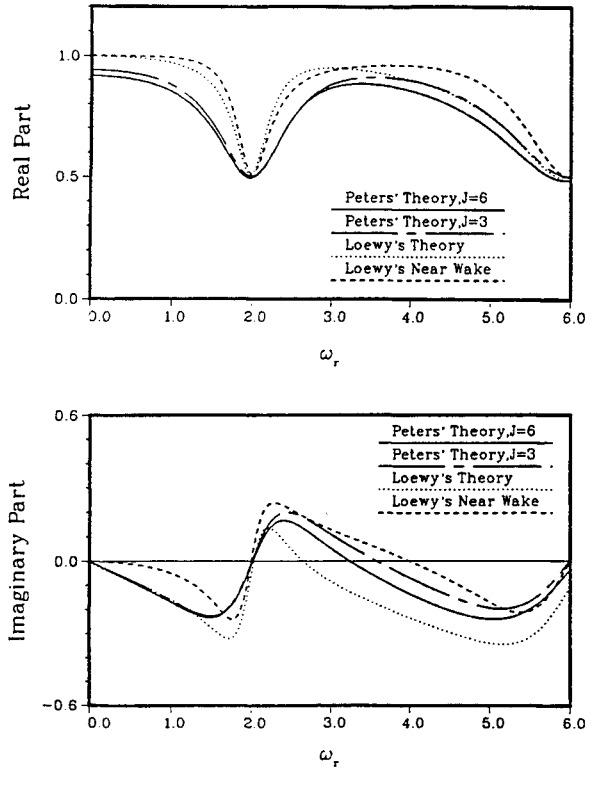

Fig. 3 Lift deficiency function, differential mode, $V = 0.05$, $Q = 4$, $\sigma = 0.061$.

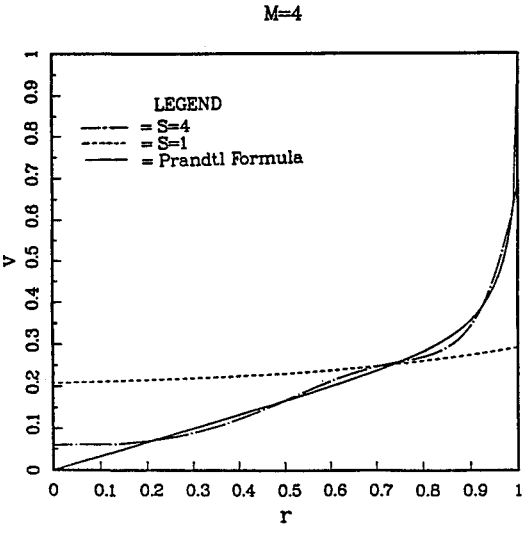

Fig. 4 Radial induced velocity distribution, axial flow.

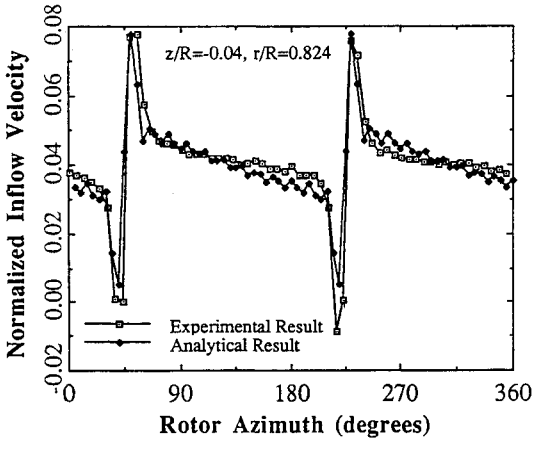

Fig. 5 Azimuthal induced velocity distribution, hover.

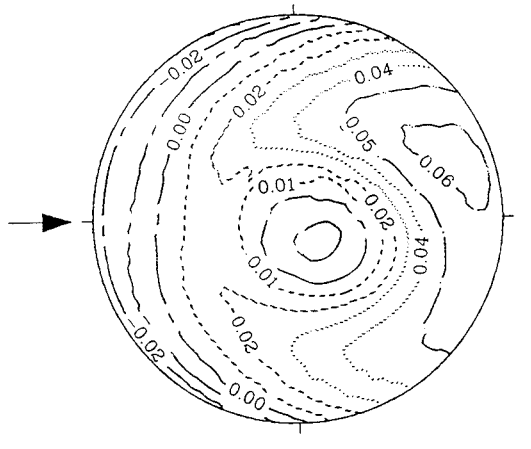

Fig. 6 Theoretical induced flow distribution, tapered blades with fuselage, $\mu = 0.15$, $C_T = 0.0064$, $\alpha = 3$ deg, $M = 4$, $S = 33$.

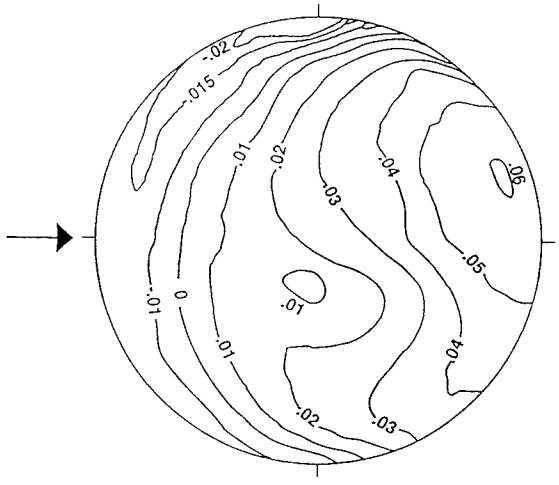

Fig. 7 Experimental induced flow distribution, tapered blades, μ = 0.15, C_T = 0.0064, α = 3 deg.

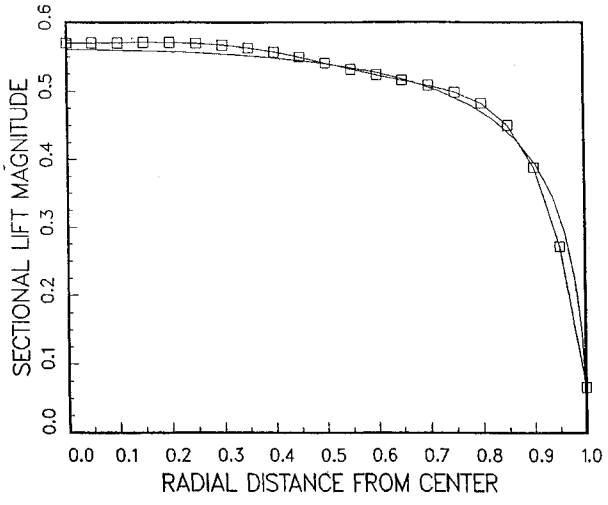

Fig. 8 Lift distribution for constant-chord wing, AR = 10, solid line = Prandtl–Glauert, squares = finite state with M = 8.

α_2^1, β_2^1). A large body of evidence shows that dynamic inflow is absolutely necessary for rotorcraft dynamic correlation.[23–27]

Summary and Conclusions

We have developed an unsteady aerodynamic theory (a generalized dynamic wake theory), based on a three-dimensional, unsteady acceleration-potential theory. The theory has the following advantages over conventional unsteady models:

1) *The model is general.* The rotor can have an arbitrary lift distribution and a finite number of blades. The rotor disc can be at any angle to the flow.

2) *The method is extremely flexible in application.* The user may choose the number of harmonics as well as the number of radial shape functions. Radial or harmonic coupling can be neglected if necessary, and the theory may be applied either as a perturbation theory or as a nonlinear theory.

3) *The method is easily used with other theories.* It may be applied either in the time domain, frequency domain, or eigenvalue domain and may be coupled to any blade-lift model (including dynamic-stall models, table look-up, and CFD computations). All that is required is the augmentation of the user's equations with additional first-order state equations.

4) *The theory recovers other theories.* Implicit in this model are the Theodorsen theory, the Loewy and Miller functions, the Prandtl/Goldstein theory, and simple dynamic inflow theory.

5) *The theory shows good correlation with all data to which it has thus far been compared.* This includes LDV measured induced-flow data, both time-averaged and time-dependent, in hover and forward flight.

The limitations of the model are that it converges slowly and so does not easily capture flow discontinuities. It cannot provide detailed information close to the blade surface such as would be necessary for modeling blade-vortex interactions or acoustical phenomena. It is basically a prescribed-wake analysis and cannot account for wake roll-up. Thus, its usefulness is in the area of rotor aeroelasticity, Q/rev vibration, and design of higher-harmonic controllers.

Appendix: Ellipsoidal Coordinate System

In the development of the dynamic wake theory, we need to define the following three coordinate systems.

Rotor Disk Cartesian Coordinate System (x, y, z)

The rotor disk coordinate system (x, y, z) has its origin located at rotor disk center, x and y axes lay in the disk with x axis pointing upstream and y axis toward starboard, and z axis downward as determined by a right-hand rule.

Wind Coordinate System (x_w, y_w, z_w)

The wind coordinate system (x_w, y_w, z_w) is obtained by a rotation of the (x, y, z) coordinates through an angle α about y (y_w) axis. The angle α is the angle between freestream and rotor disk. The transformation between these two coordinate systems can be found as

$$\begin{Bmatrix} x_w \\ y_w \\ z_w \end{Bmatrix} = \begin{bmatrix} \cos\alpha & 0 & -\sin\alpha \\ 0 & 1 & 0 \\ \sin\alpha & 0 & \cos\alpha \end{bmatrix} \begin{Bmatrix} x \\ y \\ z \end{Bmatrix} \tag{A1}$$

Ellipsoidal Coordinate System (ν, η, $\bar{\psi}$)

The ellipsoidal coordinate system (ν, η, $\bar{\psi}$) is defined such that

$$x = -\sqrt{1-\nu^2}\sqrt{1+\eta^2}\cos\bar{\psi} \tag{A2}$$

$$y = -\sqrt{1-\nu^2}\sqrt{1+\eta^2}\sin\bar{\psi} \tag{A3}$$

$$z = -\nu\eta \tag{A4}$$

It may be noted that this ν, η, $\bar{\psi}$ coordinate system will cover the entire three-dimensional space once and only once, if we restrict ν, η, and $\bar{\psi}$ to the ranges

$$-1 \le \nu \le +1 \tag{A5}$$

$$0 \le \eta < \infty \tag{A6}$$

$$0 \le \bar{\psi} < 2\pi \tag{A7}$$

Figure A1 shows the $\nu\eta\bar{\psi}$ coordinate system viewed in the xz plane. The ν = constant surfaces are hyperboloids, and the η = constant surfaces are ellipsoids, both families of surfaces being azimuthally symmetric about the z axis. $\bar{\psi}$ is the azimuthal angle measured from the negative x axis, counterclockwise looking along the plus z axis. η = 0 represents the two faces of the disc, and ν changes sign as one crosses the disc.

The inverse of the Eqs. (A2), (A3), and (A4) is

$$\nu = -(1/\sqrt{2})\mathrm{sgn}(z)\sqrt{(1-s)+\sqrt{(1-s)^2+4z^2}} \tag{A8}$$

$$\eta = -(z/\nu) \tag{A9}$$

$$\bar{\psi} = \tan^{-1}(y/-x) \tag{A10}$$

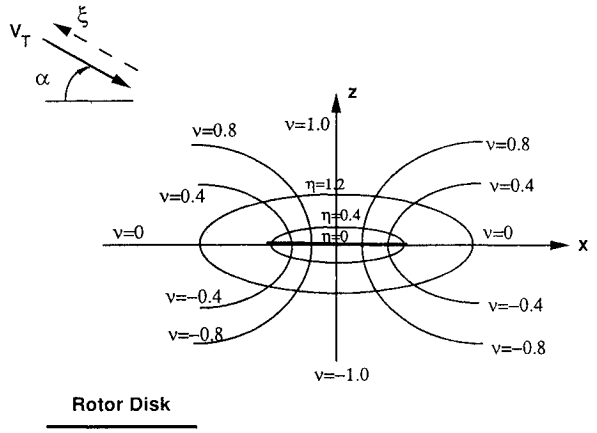

Fig. A1 Ellipsoidal coordinate system.

where

$$s = x^2 + y^2 + z^2 \tag{A11}$$

In the ellipsoidal coordinate system defined above, the Laplace's equation $\nabla^2\Phi = 0$ takes the form[28]:

$$\frac{\partial}{\partial\nu}\left[(1-\nu^2)\frac{\partial\Phi}{\partial\nu}\right] + \frac{\partial}{\partial\eta}\left[(1+\eta^2)\frac{\partial\Phi}{\partial\eta}\right] + \frac{\partial}{\partial\bar{\psi}}\left[\frac{(\nu^2+\eta^2)}{(1-\nu^2)(1+\eta^2)}\frac{\partial\Phi}{\partial\bar{\psi}}\right] = 0 \tag{A12}$$

By separation of variables, we have

$$\Phi(\nu, \eta, \bar{\psi}) = \Phi_1(\nu)\Phi_2(\eta)\Phi_3(\bar{\psi}) \tag{A13}$$

Equation (A12) can be separated into the following three equations.

$$\frac{d^2\Phi_3}{d\bar{\psi}^2} + m^2\Phi_3 = 0 \tag{A14}$$

$$\frac{d}{d\nu}\left[(1-\nu^2)\frac{d\Phi_1}{d\nu}\right] + \left[-\frac{m^2}{1-\nu^2} + n(n+1)\right]\Phi_1 = 0 \tag{A15}$$

$$\frac{d}{d\eta}\left[(1+\eta^2)\frac{d\Phi_2}{d\eta}\right] + \left[\frac{m^2}{1+\eta^2} - n(n+1)\right]\Phi_2 = 0 \tag{A16}$$

where m and n are the constants of separation. Also, we may consider m as the harmonic number and n as the radial mode number in our dynamic wake analysis. It is immediately recognized that Eqs. (A15) and (A16) are forms of Legendre's associated differential equation.[29] The $P_n^m(\nu)$ come from one of the general solutions to Eq. (A15), and $Q_n^m(i\eta)$ from a solution to Eq. (A16). The other two solutions [i.e., $P_n^m(i\eta)$, $Q_n^m(\nu)$] are abandoned because they yield an infinite pressure in the flowfield.

Acknowledgments

The theoretical developments in this article were funded by the U.S. Army Aeroflightdynamics Directorate (ATCOM), NASA Grants NAG 2-462 and NAG 2-728, Robert A. Ormiston, Technical Monitor. The applications were supported by the Army Centers of Excellence in Rotorcraft Technology Program at Georgia Institute of Technology and Washington University.

References

[1]Landgrebe, A. J., "An Analytical and Experimental Investigation of Helicopter Rotor Hover Performance and Wake Geometry Characteristics," Eustis Directorate, U.S. Army Air Mobility Research and Development Lab., USAAMRDL TR 71-24, Fort Eustis, VA, June 1971.

[2]Kocurek, J. D., and Tangler, J. L., "A Prescribed Wake Lifting Surface Hover Performance Analysis," *Journal of the American Helicopter Society*, Vol. 22, No. 1, 1977, pp. 24–35.

[3]Scully, M. P., "A Method of Computing Helicopter Vortex Wake Distortion," Massachusetts Inst. of Technology, ASRL TR138-1, Cambridge, MA, June 1967.

[4]Miller, R. H., "Rotor Blade Harmonic Air Loading," *AIAA Journal*, Vol. 2, No. 7, 1964, pp. 1254–1269.

[5]Baskin, V. E., Vil'dgrude, L. S., Vozhdayev, E. S., and Maykapar, G. I., "Theory of the Lifting Airscrew," NASA-TT F-823, Feb. 1976.

[6]Wang, S.-C., "Generalized Rotor Vortex Theory, Problems of Helicopter Rotor Aerodynamics," USSR, 1961; also, Mil, M. J., *Helicopters, Calculation and Design*, NASA TT F-494, Sept. 1967.

[7]Mangler, K. W., "Calculation of the Induced Velocity Field of a Rotor," Royal Aircraft Establishment, Rept. Aero 2247, Sept. 1948.

[8]Van Holten, T., "The Computation of Aerodynamic Loads on Helicopter Blades in Forward Flight, Using the Method of the Acceleration Potential," Technische Hogeschool Delft, Rept. VTH-189, The Netherlands, March 1975.

[9]Runyan, H. L., and Tai, H., "Application of a Lifting Surface Theory for a Helicopter in Forward Flight," *Proceedings of the 11th European Rotorcraft Forum*, London, 1985, pp. 24-1–24-18.

[10]Peters, D. A., Boyd, D. D., and He, C.-J., "Finite-State Induced Flow Model for Rotors in Hover and Forward Flight," *Journal of the American Helicopter Society*, Vol. 34, No. 4, 1989, pp. 5–17.

[11]Peters, D. A., and Su, A., "An Integrated Airloads-Inflow Model for Use in Rotor Aeroelasticity and Control Analysis," *Proceedings of the 47th Annual National Forum of the American Helicopter Society* (Phoenix, AZ), 1991, pp. 25–40.

[12]Su, A., Yoo, K. M., and Peters, D. A., "Extension and Validation of an Unsteady Wake Model for Rotors," *Journal of Aircraft*, Vol. 29, No. 3, 1992, pp. 374–383.

[13]Peters, D. A., and He, C.-J., "Correlation of Measured Induced Velocities with a Finite-State Wake Model," *Journal of the American Helicopter Society*, Vol. 36, No. 3, 1991, pp. 59–70.

[14]De Andrade, D., and Peters, D. A., "Correlation of Experimental Flap-Lag-Torsion Damping—A Case Study," *Proceedings of the 49th Annual National Forum of the American Helicopter Society* (St. Louis, MO), 1993, pp. 1011–1028.

[15]Kinner, W., "Die Kreisfirmige Tragflache auf Potentialtheorischer Grundlage," Ingenier Archive VIII Band, 1937, pp. 47–80.

[16]Schade, T., and Krrences, K., "The Oscillating Circular Airfoil on the Basis of Potential Theory," *Luftfarlforschung*, Vol. 17, Nos. 11–12, 1940, and Vol. 19, No. 8, 1942; also NACA TM 1098, Feb. 1947.

[17]Hauptman, A., and Miloh, T., "Aerodynamic Coefficients of a Circular Wing in Subsonic Flow," *Israel Journal of Technology*, Vol. 23, 1986–7, pp. 17–24.

[18]He, C.-J., "Development and Application of a Generalized Dynamic Wake Theory for Lifting Rotors," Ph.D. Dissertation, Georgia Inst. of Technology, Atlanta, GA, July 1989.

[19]Su, A., "Application of a State-Space Wake Model to Elastic Blade Flapping in Hover," Ph.D. Dissertation, Georgia Inst. of Technology, Atlanta, GA, Dec. 1989.

[20]Kline, M., *Mathematical Thought from Ancient to Modern Times*, Oxford Univ. Press, New York, 1972, p. 453.

[21]Gaonkar, G. H., McNaulty, M. J., and Nagabhushannam, J., "An Experimental and Analytical Investigation of Isolated Rotor Flap-Lag Stability in Forward Flight," *Journal of the American Helicopter Society*, Vol. 35, No. 2, 1990, pp. 25–34.

[22]Nibbelink, B. D., and Peters, D. A., "Flutter Calculations for Fixed and Rotating Wings with State-Space Inflow Dynamics," *Proceedings of AIAA/AHS/ASME Structural Dynamics and Materials Conference*, La Jolla, CA, April 1993.

[23]Ormiston, R. A., and Peters, D. A., "Hingeless Rotor Response with Nonuniform Inflow and Elastic Blade Bending," *Journal of Aircraft*, Vol. 9, No. 10, 1972, pp. 730–736.

[24]Pitt, D. M., and Peters, D. A., "Theoretical Prediction of Dynamic Inflow Derivatives," *Vertica*, Vol. 5, No. 1, 1981, pp. 21–34.

[25]Zhao, X., and Curtiss, H. C., "A Linearized Model of Helicopter Dynamics Including Correlation with Flight Test," *Proceedings of the*

Second International Conference on Rotorcraft Basic Research, Univ. of Maryland, College Park, MD, Feb. 1988.

[26]Schrage, D., Peters, D. A., Pasad, J. V. R., Stumpf, W. F., and He, C.-J., "Helicopter Stability and Control Modeling Improvements and Verification on Two Helicopters," *Proceedings of the Fourteenth European Rotorcraft Forum*, Milan, Italy, 1988, pp. 77-1–77-26 (Paper 77).

[27]Johnson, W., "Influence of Unsteady Aerodynamics on Hingeless Rotor Ground Resonance," *Journal of Aircraft*, Vol. 29, No. 9, 1982, pp. 668–673.

[28]Joglekar, M., and Loewy, R., "An Actuator-Disc Analysis of Helicopter Wake Geometry and the Corresponding Blade Response," USAAULABS TR 69-66, Dec. 1970.

[29]Lebedev, N. N., *Special Functions and Their Applications*, edited by A. S. Richard, Prentice–Hall, Englewood Cliffs, NJ, 1965, pp. 192, 193 (revised English translation)